Transient optical reflectivity from bounded nonlocal media: Normal incidence

Spiros V. Branis, K. Arya,* and Joseph L. Birman
Department of Physics, City College of the City University of New York, Convent Avenue at 138th Street, New York, New York 10031
(Received 2 August 1988)

The reflection of a finite-duration optical pulse from a semi-infinite nonlocal medium for various additional boundary conditions (ABC's) is investigated theoretically. We have obtained explicit expressions for the amplitude and phase of the transient reflected field (local and nonlocal) and evaluated them numerically for different ABC's. We predict a damped oscillatory decay in transient reflectivity (after the pulse is cut off) due to relaxation processes which cause dephasing of emitted light on a scale longer than the cutoff time of the pulse. The effects of spatial dispersion for the reflected transients associated with the light pulse are important for the laser frequency at the vicinity of an exciton-polariton resonance. For various ABC's, for the cases of CdS and CuCl semiconductors, we find quantitative differences in the magnitude of the amplitude of the transient. This can be used to analyze different ABC's experimentally.

I. INTRODUCTION

Propagation of an electromagnetic (EM) wave in a bounded nonlocal dielectric medium has attracted much attention in recent years.[1] Because of spatial dispersion, the dielectric function $\epsilon(\omega,\mathbf{k})$ has wave-vector dependence. This leads to more than one plane wave propagating inside the medium when a single plane wave is incident. One thus needs additional boundary conditions (ABC's) in addition to Maxwell boundary conditions in order to solve the reflection and transmission problem from a nonlocal medium. In semiconductors, such as CdS, CuCl, GaSe, GaS, etc., the effects of spatial dispersion become very important near the exciton resonance ω_t. Their study in various optical processes, such as reflection and transmission or Raman and Brillouin scattering, may thus provide valuable information about exciton parameters.[2]

Instead of steady-state wave, finite pulses can give additional information about spatial dispersion. For example, for EM pulses of finite duration the transient effects give rise to precursors in the transmission regime. For the local medium, the well-known Sommerfeld[3] and Brillouin[4] precursors are present, while spatial dispersion gives rise to a third precursor, namely the exciton precursor.[5] Transient optical transmission has been investigated only when the light pulse has well-defined boundaries.[6–8] Reflection from a nonlocal interface has only been studied in the steady-state regime for various angles of incident light and for various additional boundary conditions (ABC's).[9–11] Transient reflectivity from a local frequency-dispersive dielectric was considered by Elert more than 50 years ago, and more recently by Eilbeck, Fauchet, and Branis,[12] while generalization to nonlocal media was reported for the first time for normal light incidence in the case of Pekar's ABC.[13]

The purpose of this paper is to provide a detailed analysis of the effects of spatial dispersion on transient reflectivity, for various ABC's. When an electromagnetic pulse of finite duration T is incident on a nonlocal interface, the reflected field consists of the steady-state signal (of duration T) and transients arising from both the leading and the trailing pulse edges. Experimentally, it may be more convenient to look for trailing-edge transient reflectivity, since steady-state reflectivity will then not interfere with measurements. For long pulses (T greater than a few psec), transients from the two edges will be essentially decoupled and can be measured independently. In our case, we consider an incident square pulse and obtain expressions for steady-state and transient reflectivity for various ABC's. The results show that the transient reflectivity consists of a "local" part and a "nonlocal" part. We obtain expressions for local and nonlocal parts, respectively, to show the differences among the ABC's, especially close to the exciton-polariton resonance frequency ω_l, where spatial-dispersion effects are enhanced. We propose that by measuring the total transient reflectivity, it is possible to decide about the "true" ABC for the material. The local part is on the average larger than the nonlocal part at fixed time, especially close to longitudinal frequency ω_l, while the nonlocal part is enhanced at ω_t. The time oscillatory decay of both parts is also obtained, at fixed frequency. We show different oscillatory decay rates for both parts and for different ABC's. The magnitude of transient intensities should permit an experimental measurement.

The plan of the paper is as follows. In Sec. II, a review of the different ABC's is given with a discussion of the basic assumptions that underlie them. In Sec. III, an integral representation for the reflected field is obtained, by using Fourier analysis in the time domain, for semi-infinite nonlocal medium. Using a contour-integration method, expressions for the steady-state and transient parts of the reflectivity are obtained in Sec. IV. Sections V and VI deal with the "nonlocal" and "local" parts of transient reflectivity, respectively. Detailed numerical results are presented for parameters appropriate to CdS and CuCl crystals. The results for total transient

reflectivity are discussed in Sec. VII, while in Sec. VIII we summarize our results. Necessary mathematical details are presented in the Appendix.

II. REVIEW OF DIFFERENT ABC'S (REF. 14)

Simultaneously with the prediction of the existence of additional waves in spatially dispersive media, the need for more than the usual Maxwell boundary conditions was realized.

In his first paper, Pekar[15] discussed a quantum-mechanical approach to obtain an ABC. He proposed that in the nonlocal medium the exciton polarization $\mathbf{P}_{\rm exc}(\mathbf{r},t)$ satisfies the equation of motion

$$\left[-\omega_0^2+\frac{\partial^2}{\partial t^2}+b\nabla^2+\Gamma\frac{\partial}{\partial t}\right]\mathbf{P}_{\rm exc}(\mathbf{r},t)=\alpha\mathbf{E}(\mathbf{r},t)\ , \tag{2.1}$$

with $-\omega_0^2, b, \Gamma, \alpha$ being coefficients and the macroscopic field $\mathbf{E}(\mathbf{r},t)$ acting as a driving force on the exciton polarization. For harmonic plane-wave propagation in the medium in $+z$ direction (normal incidence), Eq. (2.1) leads to a macroscopic constitutive relation for $\mathbf{P}_{\rm exc}(\mathbf{r},t)$:

$$\mathbf{P}_{\rm exc}(\mathbf{k},\omega)=\chi_{\rm exc}(\mathbf{k},\omega)\mathbf{E}(\mathbf{k},\omega) \tag{2.2}$$

with

$$\chi_{\rm exc}(\mathbf{k},\omega)=\frac{\alpha}{(\omega_0^2+bk^2-\omega^2-i\Gamma\omega)}\ , \tag{2.3}$$

or by adding a background term:

$$\chi(\mathbf{k},\omega)=\chi_0+\chi_{\rm exc}(\mathbf{k},\omega)\ . \tag{2.4}$$

Equation (2.1) was solved subject to a boundary condition:

$$\mathbf{P}_{\rm exc}(\mathbf{r},t)|_\Sigma=\mathbf{0} \tag{2.5}$$

or

$$(n_1^2-\epsilon_0)E_1+(n_2^2-\epsilon_0)E_2=0\ , \tag{2.6}$$

since the polarization vanishes outside the medium, while Σ is the boundary of the medium at $z=0$. In Eq. (2.6), n_1, n_2 are the complex indices of refraction for the two propagating modes while ϵ_0 is the dielectric constant of the background. The boundary condition in Eq. (2.5) is not a mathematical consequence of the assumed susceptibility, but an assertion imposed by Pekar to complete the solution of Maxwell equations in the presence of spatial dispersion.

A few years later, Hopfield and Thomas[16] took up the ABC problem. Following somewhat along the lines of Pekar's paper they introduced the equation of motion as in Eq. (2.1) and analyzed a quantum-mechanical model which would give a Schrödinger eigenfunction for the exciton. From this eigenfunction they deduced the needed ABC (imposing a restriction that the exciton wave function should vanish on the surface of the medium) using a classical correspondence. The new ABC had the form

$$\mathbf{P}_{\rm exc}(\mathbf{r},t)+A\frac{\partial\mathbf{P}_{\rm exc}(\mathbf{r},t)}{\partial z}\bigg|_\Sigma=\mathbf{0}\ , \tag{2.7}$$

where Pekar's ABC is a particular case ($A=0$). Fuchs and Kliewer[17] derived a similar result for the optical properties of a semi-infinite electron gas; the connection between their approach and that of ABC's was elucidated by Johnson and Rimbey.[18] Kiselev[19] gave a more explicit expression for $A=\gamma c/\omega$, where γ is some phenomenological constant or function of frequency. In terms of electric fields, Eq. (2.7) is written as follows:

$$(1+i\gamma n_1)(n_1^2-\epsilon_0)E_1+(1+i\gamma n_2)(n_2^2-\epsilon_0)E_2=0\ . \tag{2.8}$$

Birman and Sein,[20] Maradudin and Mills,[21] and Agrawal *et al.*[22] independently used Maxwell equations in a phenomenological way to propose a different ABC. Their contribution was based on the fact that by choosing a nonlocal susceptibility model, an ABC can be derived through either an integral or differential equation formalism of electrodynamics for nonlocal media, without any additional assumption. By using Eq. (2.4) (dielectric approximation) the result for an ABC is

$$\frac{\partial\mathbf{P}_{\rm exc}(\mathbf{r},t)}{\partial z}+ik_+\mathbf{P}_{\rm exc}(\mathbf{r},t)\bigg|_\Sigma=\mathbf{0} \tag{2.9}$$

or

$$\frac{E_1}{n_1-n_+}+\frac{E_2}{n_2-n_+}=0 \tag{2.10}$$

with

$$k_+^2=n_+^2\frac{\omega^2}{c^2}=\frac{m^*}{\hbar\omega_t}(\omega^2-\omega_t^2+i\omega\Gamma)\ , \tag{2.11}$$

where m^* is the effective exciton-polariton mass, ω_t is the transverse exciton angular frequency, Γ is a phenomenological damping constant, and n_+ is the refractive index for the lower polariton mode for $\omega\gg\omega_t$. This approach is totally macroscopic.

Zeyher *et al.*[23] gave a microscopic determination of ABC's. The fundamental assumption about the physics of exciton-polariton reflection at the crystal surface decides for the different ABC's. The wave function for the exciton-polariton center-of-mass motion is approximated as follows:

$$\Psi_{\mathbf{k}}(\mathbf{r},\omega)=\Theta(z)[\exp(ik_z z)+R_{\rm exc}\exp(-ik_z z)]\times\exp(i\mathbf{k}_\parallel\cdot\mathbf{r})\ , \tag{2.12}$$

where $R_{\rm exc}$ is the exciton reflection coefficient. For $R_{\rm exc}=0$, one obtains exactly the Birman-Sein ABC Eq. (2.10). The physical meaning of the zero exciton reflection coefficient corresponds to the translationally invariant susceptibility or dielectric approximation. For $R_{\rm exc}=-1$, this corresponds to Frenkel or tight-binding excitons, which are totally reflected by the crystal surface. In this case, the relative electron-hole motion is not affected by the process. One can obtain Pekar's ABC Eq. (2.5) for $\chi_0=0$. The last case, $R_{\rm exc}=+1$, corresponds to

Wannier excitons case. This case was treated first by Ting *et al.* (1975) (Ref. 24) and one obtains a new ABC (Ting's ABC):

$$\left.\frac{\partial \mathbf{P}_{\rm exc}(\mathbf{r},t)}{\partial z}\right|_{\Sigma}=0 \tag{2.13}$$

or

$$n_1(n_1^2-\epsilon_0)E_1+n_2(n_2^2-\epsilon_0)E_2=0\ . \tag{2.14}$$

III. INTEGRAL REPRESENTATION FOR THE REFLECTED FIELD

We consider a semi-infinite nonlocal medium occupying the half-space $z>L$ with $z<L$ being vacuum (see Fig. 1). A detector is placed at $z=0$. We assume that a normally incident laser pulse corresponds to a linearly, polarized, monochromatic plane-wave field. For a square pulse of unit intensity and duration T at frequency ω_0, the electric field at the plane $z=0$ is given by

$$E_I(0,t)=\sin(\omega_0 t)[\Theta(t)-\Theta(t-T)]\ , \tag{3.1}$$

where $\Theta(t)$ is the Heaviside step function.

For laser frequency near the exciton resonance, the coupling of an exciton state to a photon produces an exciton polariton. Spatial dispersion or the nonlocality of the medium corresponds to the center-of-mass motion of the exciton polariton. A generalized classical Lorenz oscillator model takes for dielectric function

$$\epsilon(\mathbf{k},\omega)=\epsilon_0+4\pi\chi(\mathbf{k},\omega)$$

$$=\epsilon_0+\frac{4\pi\alpha_0\omega_t^2}{\omega_t^2-\omega^2-i\omega\Gamma+(\hbar\omega_t/m^*)k^2}\ , \tag{3.2}$$

where ϵ_0 is the backround dielectric constant, α_0 is the oscillator strength, m^* is the effective exciton-polariton mass, ω_t is the transverse exciton-polariton frequency, while Γ is a phenomenological damping constant which has been taken constant in the vicinity of ω_t. In reality, for CdS (Refs. 25 and 26) and CuCl (Ref. 27) crystals, Γ depends on the frequency. Expression (3.2) produces a translationally invariant real-space dielectric function $\epsilon(\mathbf{r}-\mathbf{r}',\omega)$ after Fourier transformation.

For normal incidence, the amplitude reflection coefficient is given by[28,29]

$$\rho(\omega)=\frac{1-\bar{n}(\omega)}{1+\bar{n}(\omega)}\ , \tag{3.3}$$

where $\bar{n}(\omega)$ is the effective refractive index of the nonlocal medium and for different ABC's has the following forms.

For Pekar,

$$\bar{n}(\omega)=\frac{n_1n_2+\epsilon_0}{n_1+n_2}\ , \tag{3.4a}$$

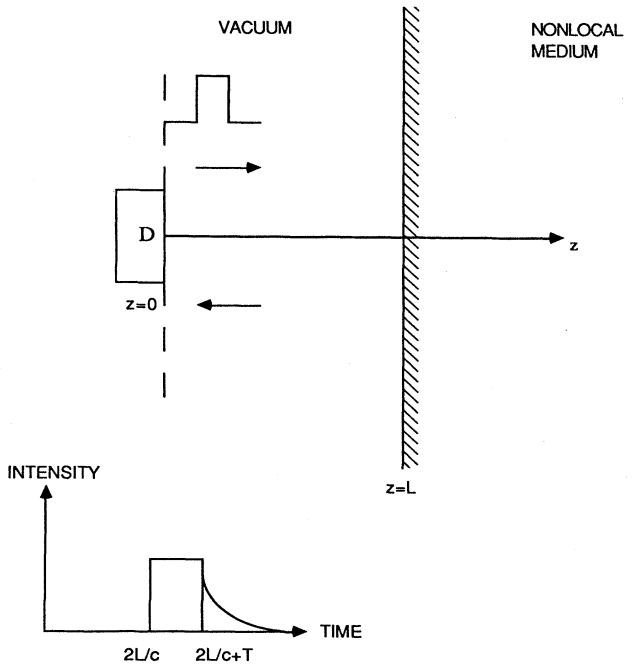

FIG. 1. Schematic illustration of the geometry and the notation used. At time $t=0$, a square pulse of duration T is emitted from the plane $z=0$ where a detector is placed to monitor the reflectivity. For $2L/c<t<(2L/c+T)$ the steady-state signal is detected and for $\tau=t-2L/c-T\geq 0$ the transient signal is detected.

for Birman,

$$\bar{n}(\omega)=n_1+n_2-n_+\ , \tag{3.4b}$$

for Ting,

$$\bar{n}(\omega)=\frac{n_1n_2(n_1+n_2)}{(n_1^2+n_2^2+n_1n_2)-\epsilon_0}\ , \tag{3.4c}$$

for Kiselev,

$$\bar{n}(\omega)=\frac{\epsilon_0+n_1n_2+i\gamma n_1n_2(n_1+n_2)}{n_1+n_2+i\gamma(n_1^2+n_2^2+n_1n_2-\epsilon_0)}\ , \tag{3.4d}$$

and n_1,n_2 are the solutions of the implicit relation

$$n_j=+[\epsilon(k_j,\omega)]^{1/2},\quad k_j=n_j\omega/c,\quad j=1,2\ . \tag{3.5}$$

Because of the linearity of the problem, we may time Fourier analyze Eq. (3.1) and treat each frequency component by dispersion theory. The reflected field is obtained as a superposition of the reflected components and can be written as the frequency integral

$$E_R(0,t,\omega_0)=\lim_{\eta\to 0}\mathrm{Re}\left\{\frac{1}{2\pi}\int_{-\infty}^{+\infty}d\omega\frac{\rho(\omega)}{\omega_0-\omega-i\eta}\{1-\exp[i(\omega-\omega_0)T]\}\exp\left[-i\omega\left[t-\frac{2L}{c}\right]\right]\right\}\ , \tag{3.6}$$

where the time delay $2L/c$ corresponds to a round trip between $z=0$ and $z=L$.

IV. STEADY-STATE AND TRANSIENT REFLECTIVITY

The reflected field, in Eq. (3.6), can be separated into steady-state and transient parts, after removing the harmonic time dependence $\exp(-i\omega t)$. The steady-state part gives rise to a reflected pulse (of duration T) whose leading and trailing edges contain the rapidly-time-varying transient contributions. The integral in Eq. (3.6) is evaluated in the complex ω plane using the method of contour integration. Using Eq. (3.3) in Eq. (3.6), the integrand is found to have the following singularities which are the same for all four ABC's: (i) a simple pole at $\omega_0-i\eta$, (ii) four branch points ω_j $(j=1,4)$ in the lower half-plane, (iii) two branch points ω_5 and ω_6 in the upper half-plane. All six branch points correspond to branch-point singularities of the complex functions $n_1(\omega), n_2(\omega)$. (iv) For Birman's ABC, there are two additional branch points ω_7 and ω_8 in the lower half-plane, corresponding to the branch-point singularities of the complex function $n_+(\omega)$.

The explicit expressions for the location of these branch points are obtained using Eqs. (3.2) and (3.5) and are given by (see details in the Appendix)

$$\omega_{1,2}=-i\tfrac{1}{2}\Gamma\pm\left[\omega_t^2\left[1+\frac{\beta^2}{\epsilon_0}\right]-\tfrac{1}{4}\Gamma^2\right]^{1/2}, \tag{4.1}$$

$$\omega_{3,4}=(1-\delta^2\epsilon_0)^{-1}\{-i(\tfrac{1}{2}\Gamma+\beta\delta\omega_t) \pm[\omega_t^2(1-\delta^2\epsilon_0) -(\beta\delta\omega_t+\tfrac{1}{2}\Gamma)^2]^{1/2}\}, \tag{4.2}$$

$$\omega_{5,6}=(1-\delta^2\epsilon_0)^{-1}\{i(\beta\delta\omega_t-\tfrac{1}{2}\Gamma) \pm[\omega_t^2(1-\delta^2\epsilon_0) -(-\beta\delta\omega_t+\tfrac{1}{2}\Gamma)^2]^{1/2}\}, \tag{4.3}$$

$$\omega_{7,8}=-i\frac{\Gamma}{2}\pm(\omega_t^2-\tfrac{1}{4}\Gamma^2)^{1/2}, \tag{4.4}$$

where

$$\beta=(4\pi\alpha_0)^{1/2}, \quad \delta=\left[\frac{\hbar\omega_t}{m^*c^2}\right]^{1/2}. \tag{4.5}$$

Note that the dimensionless parameter δ is a measure of the extent of nonlocality of the medium (spatial-dispersion coefficient). We also assume $\Gamma<2\beta\delta\omega_t$, i.e., we exclude very heavily damped exciton polaritons.

One can simplify Eqs. (4.1)–(4.4) by noting the fact that for most materials like CdS, CuCl, GaSe, and GaS, the parameters $\delta=(\hbar\omega_t/m^*c^2)^{1/2}$, $p=\beta^2/2\epsilon_0$, and Γ/ω_t are small ($\leq 10^{-3}$), so that it is sufficient to retain only lower order terms in δ, p and Γ/ω_t. Thus we obtain

$$\omega_{1,2}=-i\tfrac{1}{2}\Gamma\pm\omega_t(1+p), \tag{4.6}$$

$$\omega_{3,4}=-i(\tfrac{1}{2}\Gamma+\beta\delta\omega_t)\pm\omega_t, \tag{4.7}$$

$$\omega_{5,6}=i(\beta\delta\omega_t-\tfrac{1}{2}\Gamma)\pm\omega_t, \tag{4.8}$$

$$\omega_{7,8}=-i\tfrac{1}{2}\Gamma\pm\omega_t. \tag{4.9}$$

For $t<2L/c$ we close the contour in the upper half-plane which is chosen so as to exclude the branch-cut line joining ω_5 and ω_6. An evaluation of the integral in Eq. (3.6) shows that the branch points ω_5 and ω_6 contribute in such a manner that $E_R(t<2L/c)=0$ as required by causality.

For $t\geq 2L/c$, we close the contour in the lower half-plane. The four branch points $\omega_{1,2},\omega_{3,4}$ for the case of the ABC's of Pekar, Ting, and Kiselev and the six branch points $\omega_{1,2},\omega_{3,4},\omega_{7,8}$ for Birman's ABC are joined by branch-cut lines and the resulting contour for both cases is shown in Figs. 2(a) and 2(b). Evaluation of the integral in Eq. (3.6) is lengthy, although straightforward. Algebraic details are presented in the Appendix. Here we note that the reflected field is found to consist of three parts [see Eq. (A20)]:

$$E_R(0,t,\omega_0)=\mathrm{Re}[\tilde{E}_S(t)+\tilde{E}_L(t)+\tilde{E}_{\mathrm{NL}}(t)]. \tag{4.10}$$

The simple pole at ω_0-$i\eta$ contributes to the steady-state reflected field $\tilde{E}_S(t)$. The four branch points (or the six ones for Birman's ABC) contribute to the transient reflected field which consists of a local part $\tilde{E}_L(t)$ and a nonlocal part $\tilde{E}_{\mathrm{NL}}(t)$. Although $\tilde{E}_S(t)$ and $\tilde{E}_L(t)$ both are affected by spatial dispersion, $\tilde{E}_{\mathrm{NL}}(t)$ arises solely from it and vanishes as $\delta\to 0$ $(m^*\to\infty)$. Further, in the limit of $\delta\to 0$, $\tilde{E}_S(t)$ and $\tilde{E}_L(t)$ reduce to the previously obtained results.[12] We now consider the steady-state and transient parts of the reflected field separately.

A. Steady-state reflectivity

Using Eq. (A21) from the Appendix, $\tilde{E}_S(t)$ is given by

$$\tilde{E}_S(t)=-i\rho(\omega_0)\exp\left[-i\omega_0\left[t-\frac{2L}{c}\right]\right] \tag{4.11}$$

for all ABC's for $2L/c<t<(2L/c+T)$ and zero otherwise. After an initial delay, a reflected square pulse of duration T arrives at the plane $z=0$. In Figs. 3 and 4 we have shown the reflectivity $|R_0|^2=|\rho(\omega_0)|^2$ as a function of ω_0/ω_t in the vicinity of exciton-polariton resonance for parameters appropriate to CdS (Ref. 13) and CuCl (Ref. 27) crystals, for all ABC's, respectively. Reflectivity for a local medium ($\delta=0$) is shown by a solid line for comparison. We notice that the main effect of spatial dispersion is to reduce the reflectivity peak height for all ABC's but more drastically for Pekar's and Birman's ABC.

B. Transient reflectivity

Transient reflectivity consists of a "local" part and a "nonlocal" part:

$$\tilde{E}_T(t)=\tilde{E}_L(t)+\tilde{E}_{\mathrm{NL}}(t), \tag{4.12}$$

where the "local" part is what remains in $E_L(\tau)$ when $\delta\to 0$, and from Eq. (A22)

$$\tilde{E}_T(t)=[E_j(t-2L/c)\Theta(t-2L/c) - \exp(-i\omega_0 T)E_j(t-2L/c-T) \times\Theta(t-2L/c-T)] \quad (4.13)$$

for $j=L$ and NL and $E_L(\tau)$ and $E_{\rm NL}(\tau)$ are given by Eqs. (A16)–(A19). The two terms in Eq. (4.13) correspond to transients arising from the leading and trailing pulse edges, respectively. If the pulse duration T is longer than the effective time during which transients significantly contribute, leading-and trailing-edge transients will not interfere and can be considered independently. Up to a constant phase factor, transients from both edges are identical in form and magnitude and are governed by $E_j(\tau)$. Experimentally, it may be more convenient to look for trailing-edge transients which appear just after the reflected pulse is cut off at $t=2L/c+T$. Using Eqs. (A3) and (A12) in Eq. (A23), the local part of the transient reflectivity is found to be given by

$$E_L(\tau)=\exp(-i\omega_t\tau)\exp(-\tfrac{1}{2}\Gamma\tau)\left[\frac{p\omega_t}{2\pi}\right] \times\int_0^1\frac{[\rho(n_1,n_2)-\rho(-n_1,n_2)]}{(\omega_t-\omega_0+p|\omega_t|u-i\frac{1}{2}\Gamma)} \times\exp(-ip\omega_t\tau u)du+\cdots \quad (4.14)$$

for the ABC's of Pekar, Ting, and Kiselev, and by using Eqs. (A3) and (A14) in Eq. (A25),

$$E_L(\tau)=\exp(-i\omega_t\tau)\exp(-\tfrac{1}{2}\Gamma\tau)\left[\frac{p\omega_t}{2\pi}\right] \times\int_0^1\frac{[\rho(n_1,n_2,n_+)-\rho(-n_1,n_2,n_+)]}{(\omega_t-\omega_0+p|\omega_t|u-i\frac{1}{2}\Gamma)} \times\exp(-ip\omega_t\tau u)du+\cdots \quad (4.15)$$

for Birman's ABC where the ellipsis represents a similar expression obtained by $\omega_t\to-\omega_t$. Here, dependence of $\rho(\omega)$ on the refractive indices n_1 and n_2 plus its dependence on n_+ for Birman's ABC is explicitly shown and n_1, n_2, and n_+ are to be evaluated at frequency $\omega=\omega_t+p\omega_t u-i\frac{1}{2}\Gamma$. As a reminder, $p=2\pi\alpha_0/\epsilon_0=(\omega_l-\omega_t)/\omega_t$.

It is easy to verify that Eqs. (4.13) and (4.14) reduce to Elert's result[12] in the limit of infinite exciton mass $\delta\to0$. This follows by noting that when $\delta\to0$, $\bar{n}=n_1$ for all ABC's and the term in square brackets in Eqs. (4.13) and (4.14) reduces to $-4n_1/(1-n_1^2)$.

The nonlocal part is given by Eq. (A24) which together with (A3) and (A12) becomes

$$E_{\rm NL}(\tau)=\exp(-i\omega_t\tau)\exp(-\tfrac{1}{2}\Gamma\tau)\left[\frac{i\beta\delta\omega_t}{2\pi}\right] \times\left[\int_0^1\frac{[\rho(n_1,n_2)-\rho(-n_1,n_2)]}{(\omega_t-\omega_0-i\beta\delta|\omega_t|u-i\frac{1}{2}\Gamma)}\exp(-\beta\delta|\omega_t|\tau u)du+\cdots + \int_1^\infty\frac{[\rho(n_1,n_2)-\rho(-n_2,n_1)]}{(\omega_t-\omega_0-i\beta\delta|\omega_t|u-i\frac{1}{2}\Gamma)}\exp(-\beta\delta|\omega_t|\tau u)du+\cdots\right] \quad (4.16)$$

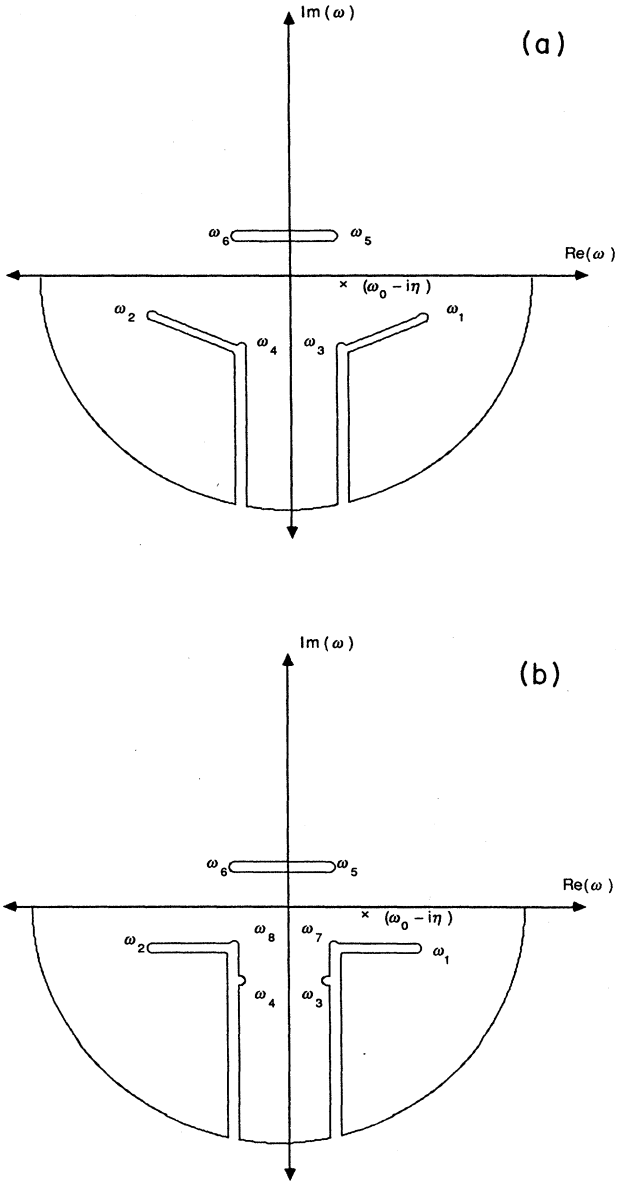

FIG. 2. (a) Schematic illustration of the contour in the complex ω needed to evaluate the reflected for Pekar, Ting, and Kiselev's ABC. A pole at $\omega-i\eta$ and six branch-point singularities ω_j, $j=1$ to 6 give rise to the steady-state and transient reflectivity, respectively. (b) Schematic illustration of the contour in the complex ω plane needed to evaluate the reflected for Birman's ABC. A pole at $\omega-i\eta$ and eight branch-point singularities ω_j, $j=1$ to 8, give rise to the steady-state and transient reflectivity, respectively.

for the ABC's of Pekar, Ting, and Kiselev, and from Eq. (A24) with (A14) and (A3)

$$E_{\mathrm{NL}}(\tau)=\exp(-i\omega_t\tau)\exp(-\tfrac{1}{2}\Gamma\tau)\left[\frac{i\beta\delta\omega_t}{2\pi}\right]\times\left[\int_0^1\frac{[\rho(n_1,n_2,n_+)-\rho(-n_1,n_2,-n_+)]}{(\omega_t-\omega_0-i\beta\delta|\omega_t|u-i\frac{1}{2}\Gamma)}\exp(-\beta\delta|\omega_t|\tau u)du+\cdots+\int_1^\infty\frac{[\rho(n_1,n_2,n_+)-\rho(-n_2,n_1,-n_+)]}{(\omega_t-\omega_0-i\beta\delta|\omega_t|u-i\frac{1}{2}\Gamma)}\exp(-\beta\delta|\omega_t|\tau u)du+\cdots\right] \tag{4.17}$$

for Birman's ABC where the ellipses represent a similar expression obtained by $\omega_t\rightarrow-\omega_t$. Here, dependence of $\rho(\omega)$ on the refractive indices n_1 and n_2 plus its dependence on n_+ for Birman's ABC is explicitly shown and n_1, n_2, and n_+ are evaluated at frequency $\omega=\omega_t-i\beta\delta\omega_t u-i\frac{1}{2}\Gamma$. Note that $\tilde{E}_{\mathrm{NL}}(t)$ is proportional to the spatial-dispersion parameter δ and vanishes for the case of local medium in the limit of infinite exciton mass ($\delta=0$).

Equations (4.13)–(4.17) give the total transient reflected field associated with a square pulse of duration T. In the following, we focus our attention on transients arising from the trailing pulse edge and set $\tau=t-2L/c-T$. For $T>$ a few psec, leading-edge transients would die out before the trailing edge of the pulse arrives and therefore

$$\tilde{E}_j(\tau)\cong-\exp(-i\omega_0T)E_j(\tau)\ , \tag{4.18}$$

where $\tau>0$ and $j=L$ and NL.

Since the transient effects are expected to be important only in the immediate vicinity of an exciton-polariton resonance, we shall assume that the laser frequency $\omega_0\approx\omega_t$. Under near-resonance conditions, the second term in Eqs. (4.14) and (4.15), and the last two terms in Eqs. (4.16) and (4.17) will not contribute significantly and henceforth will be neglected. It may be noted that these terms arise from the branch points lying in the third quadrant of the complex ω plane [see Figs. 2(a) and 2(b)]. In the next two sections we consider the nonlocal and local parts of transient reflectivity separately.

V. SPATIAL-DISPERSION-INDUCED TRANSIENT REFLECTIVITY

In this section we simplify the nonlocal part of transient reflectivity [Eqs. (4.16) and (4.17)] and discuss various features numerically. For this purpose we need to evaluate n_1, n_2, and n_+ at frequency $\omega=\omega_t-i\beta\delta\omega_t u-i\frac{1}{2}\Gamma$. Using Eqs. (A4)–(A6) to the leading order in δ we obtain

$$n_{2,1}=+[a\pm(a^2-\epsilon_0 b)^{1/2}]^{1/2}\ , \tag{5.1}$$

$$n_+=+(2a-\epsilon_0)^{1/2}\ , \tag{5.2}$$

where

$$a\cong\left[\frac{\epsilon_0}{2}-\frac{i\beta u}{\delta}\right],\quad b\cong-\frac{\beta^2}{(\epsilon_0\delta^2)}\ . \tag{5.3}$$

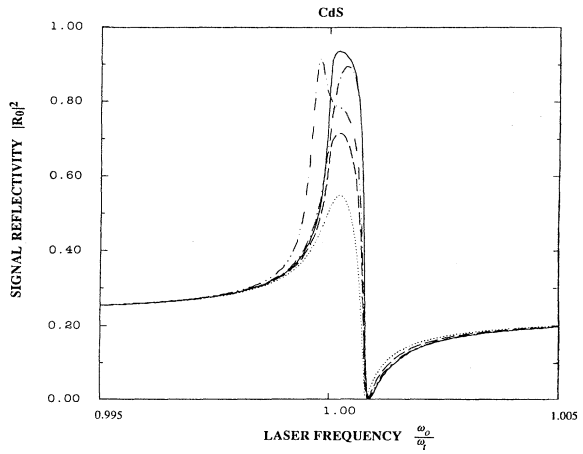

FIG. 3. Resonance enhancement of steady-state reflectivity $|R_0|^2$ which persists for $2L/c<t(2L/c+T)$. The parameters are chosen appropriate to a CdS crystal with $\epsilon_0=8$, $\hbar\omega_t=2.55$ eV, $m^*=0.9m_e$, $\Gamma/\omega_t=5\times10^{-5}$, $\beta^2=0.0125$, and $\gamma=10^{-1}$. For comparison each curve is represented by an ABC as follows: Local optics, ——; Pekar, · · · ·; Birman, — — —; Ting, —·—·—·; Kiselev, – · · – · · – · · –.

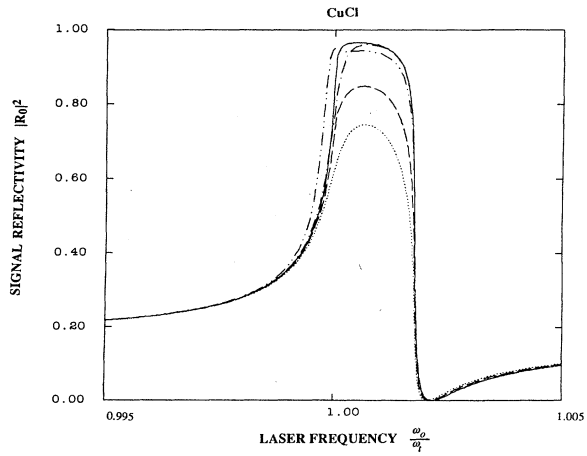

FIG. 4. Resonance enhancement of steady-state reflectivity $|R_0|^2$ which persists for $2L/c<t<(2L/c+T)$. The parameters are chosen appropriate to a CuCl crystal with $\epsilon_0=5.59$, $\hbar\omega_t=3.2022$ eV, $m^*=2.3m_e$, $\Gamma/\omega_t=5\times10^{-5}$, $\beta^2=0.0199$, and $\gamma=10^{-1}$. For comparison each curve is represented by an ABC as follows: Local optics, ——; Pekar, · · · ·; Birman, — — —; Ting, —·—·—·; Kiselev – · · – · · – · · –.

Substituting Eq. (5.3) in (5.1) and (5.2) and assuming $\epsilon_0\delta/2\beta \ll 1$, we obtain

$$n_1 = -i\left[\frac{\beta}{\delta}\right]^{1/2}\exp\left[\frac{i\theta}{2}\right], \tag{5.4}$$

$$n_2 = \left[\frac{\beta}{\delta}\right]^{1/2}\exp\left[-\frac{i\theta}{2}\right], \tag{5.5}$$

for $0 \le u \le 1$, where $\theta = \sin^{-1}u$ and

$$n_1 = \left[\frac{\beta}{\delta}\right]^{1/2}\exp\left[-\frac{i\pi}{4}\right]\exp\left[-\frac{z}{2}\right], \tag{5.6}$$

$$n_2 = \left[\frac{\beta}{\delta}\right]^{1/2}\exp\left[-\frac{i\pi}{4}\right]\exp\left[\frac{z}{2}\right], \tag{5.7}$$

for $u > 1$, where $u = \cosh z$, while

$$n_+ = \left[\frac{2\beta}{\delta}\right]^{1/2}\exp\left[-\frac{i\pi}{4}\right]\sqrt{u} \tag{5.8}$$

for every $u \ge 0$.

Using Eqs. (3.4) and (5.4)–(5.8) the effective refractive index for each ABC is found to be given by

$$\bar{n}(n_1,n_2) = \exp\left[-\frac{i\pi}{4}\right]\left[\frac{\beta}{2\delta}\right]^{1/2}(1+u)^{-1/2}, \tag{5.9a}$$

$$\bar{n}(-n_1,n_2) = \exp\left[\frac{i\pi}{4}\right]\left[\frac{\beta}{2\delta}\right]^{1/2}(1-u)^{-1/2}, \tag{5.9b}$$

$$\bar{n}(-n_2,n_1) = \exp\left[-\frac{i\pi}{4}\right]\left[\frac{\beta}{2\delta}\right]^{1/2}(u-1)^{-1/2}, \tag{5.9c}$$

for Pekar's ABC,

$$\bar{n}(n_1,n_2,n_+) = \left[\frac{2\beta}{\delta}\right]^{1/2}\exp\left[-\frac{i\pi}{4}\right](\sqrt{1+u}-\sqrt{u}), \tag{5.10a}$$

$$\bar{n}(-n_1,n_2,-n_+) = \left[\frac{2\beta}{\delta}\right]^{1/2}\exp\left[-\frac{i\pi}{4}\right]\times(i\sqrt{1-u}+\sqrt{u}), \tag{5.10b}$$

$$\bar{n}(-n_2,n_1,-n_+) = \left[\frac{2\beta}{\delta}\right]^{1/2}\exp\left[-\frac{i\pi}{4}\right]\times(-\sqrt{u-1}+\sqrt{u}) \tag{5.10c}$$

for Birman's ABC,

$$\bar{n}(n_1,n_2) = \left[\frac{2\beta}{\delta}\right]^{1/2}\exp\left[-\frac{i\pi}{4}\right]\frac{\sqrt{1+u}}{(2u+1)}, \tag{5.11a}$$

$$\bar{n}(-n_1,n_2) = \left[\frac{2\beta}{\delta}\right]^{1/2}\exp\left[\frac{i\pi}{4}\right]\frac{\sqrt{1-u}}{(1-2u)}, \tag{5.11b}$$

$$\bar{n}(-n_2,n_1) = \left[\frac{2\beta}{\delta}\right]^{1/2}\exp\left[-\frac{i\pi}{4}\right]\frac{\sqrt{u-1}}{(2u-1)}, \tag{5.11c}$$

for Ting's ABC, and

$$\bar{n}(n_1,n_2) = \left[\frac{\beta}{2\delta}\right]^{1/2}\left[\frac{\exp\left[-\frac{i\pi}{4}\right]+\gamma\left[\frac{2\beta}{\delta}\right]^{1/2}\sqrt{1+u}}{\sqrt{1+u}+i\gamma\exp\left[-\frac{i\pi}{4}\right]\left[\frac{\beta}{2\delta}\right]^{1/2}(1+2u)}\right], \tag{5.12a}$$

$$\bar{n}(-n_1,n_2) = \left[\frac{\beta}{2\delta}\right]^{1/2}\left[\frac{\exp\left[\frac{i\pi}{4}\right]-\gamma\left[\frac{2\beta}{\delta}\right]^{1/2}\sqrt{1-u}}{\sqrt{1-u}+i\gamma\exp\left[\frac{i\pi}{4}\right]\left[\frac{\beta}{2\delta}\right]^{1/2}(1-2u)}\right], \tag{5.12b}$$

$$\bar{n}(-n_2,n_1) = \left[\frac{\beta}{2\delta}\right]^{1/2}\left[\frac{\exp\left[-\frac{i\pi}{4}\right]-\gamma\left[\frac{2\beta}{\delta}\right]^{1/2}\sqrt{u-1}}{\sqrt{u-1}-i\gamma\exp\left[-\frac{i\pi}{4}\right]\left[\frac{\beta}{2\delta}\right]^{1/2}(2u-1)}\right], \tag{5.12c}$$

for Kiselev's ABC.

Equations (3.3) and (5.9)–(5.12) are used to evaluate the integrands in Eqs. (4.16) and (4.17). By assuming $(\beta/\delta) \gg 1$ and using Eq. (4.18), $E_{\rm NL}(\tau)$ has the form

$$\mathrm{Re}[E_{\rm NL}(\tau)] = |R_1(\tau)|\sin(\omega_t\tau-\phi_1), \tag{5.13}$$

where $R_1(\tau) = |R_1(\tau)|\exp[i\phi_1(\tau)]$ is given by

$$R_1(\tau)=i\exp(-i\omega_t\tau)\exp(-\tfrac{1}{2}\Gamma\tau)\left[\frac{2\beta\delta^3}{\pi^2}\right]^{1/2}\exp\left[\frac{i\pi}{4}\right]$$
$$\times\left[\int_0^1 du\frac{\exp(-\beta\delta\omega_t\tau u)}{(\omega_t-\omega_0-i\beta\delta\omega_t u-i\frac{1}{2}\Gamma)}\left[\frac{\sqrt{1+u}+i\sqrt{1-u}}{1+\left[\frac{2\delta}{\beta}\right]^{1/2}\exp\left[\frac{i\pi}{4}\right](\sqrt{1+u}-i\sqrt{1-u})}\right]\right.$$
$$\left.+\int_1^\infty du\frac{\exp(-\beta\delta\omega_t\tau u)}{(\omega_t-\omega_0-i\beta\delta\omega_t u-i\frac{1}{2}\Gamma)}\left[\frac{\sqrt{u+1}-\sqrt{u-1}}{1+\left[\frac{2\delta}{\beta}\right]^{1/2}\exp\left[\frac{i\pi}{4}\right](\sqrt{u+1}+\sqrt{u-1})}\right]\right] \tag{5.14}$$

for Pekar's ABC,

$$R_1(\tau)=i\exp(-i\omega_t\tau)\exp(-\tfrac{1}{2}\Gamma\tau)\left[\frac{\beta\delta^3}{2\pi^2}\right]^{1/2}\exp\left[\frac{i\pi}{4}\right]$$
$$\times\left[\int_0^1 du\frac{\exp(-\beta\delta\omega_t\tau u)}{(\omega_t-\omega_0-i\beta\delta\omega_t u-i\frac{1}{2}\Gamma)}\left[\frac{\sqrt{1+u}+i\sqrt{1-u}}{1+\left[\frac{2\delta}{\beta}\right]^{1/2}\exp\left[\frac{i\pi}{4}\right](\sqrt{1+u}-i\sqrt{1-u}+2\sqrt{u})}\right]\right.$$
$$\left.+\int_1^\infty du\frac{\exp(-\beta\delta\omega_t\tau u)}{(\omega_t-\omega_0-i\beta\delta\omega_t u-i\frac{1}{2}\Gamma)}\left[\frac{\sqrt{u+1}-\sqrt{u-1}}{1+\left[\frac{2\delta}{\beta}\right]^{1/2}\exp\left[\frac{i\pi}{4}\right](\sqrt{u+1}+\sqrt{u-1}+2\sqrt{u})}\right]\right] \tag{5.15}$$

for Birman's ABC,

$$R_1(\tau)=i\exp(-i\omega_t\tau)\exp(-\tfrac{1}{2}\Gamma\tau)\left[\frac{\beta\delta^3}{2\pi^2}\right]^{1/2}\exp\left[\frac{i\pi}{4}\right]$$
$$\times\left[\int_0^1 du\frac{\exp(-\beta\delta\omega_t\tau u)}{(\omega_t-\omega_0-i\beta\delta\omega_t u-i\frac{1}{2}\Gamma)}F_1(u)+\int_1^\infty du\frac{\exp(-\beta\delta\omega_t\tau u)}{(\omega_t-\omega_0-i\beta\delta\omega_t u-i\frac{1}{2}\Gamma)}F_2(u)\right], \tag{5.16}$$

where

$$F_1(u)=\frac{(1+2u)\sqrt{1-u}+i\sqrt{1+u}\,(1-2u)}{(1-u^2)^{1/2}+\left[\frac{\delta}{2\beta}\right]^{1/2}\exp\left[\frac{i\pi}{4}\right][(1+2u)\sqrt{1-u}-i\sqrt{1+u}\,(1-2u)]}$$

and

$$F_2(u)=\frac{(2u+1)\sqrt{u-1}-\sqrt{u+1}(2u-1)}{(u^2-1)^{1/2}+\left[\frac{\delta}{2\beta}\right]^{1/2}\exp\left[\frac{i\pi}{4}\right][(1+2u)\sqrt{u-1}+\sqrt{u+1}(2u-1)]}$$

for Ting's ABC, and

$$R_1(\tau)=\exp(-i\omega_t\tau)\exp(-\tfrac{1}{2}\Gamma\tau)\left[\frac{i\beta\delta\omega_t}{2\pi}\right]$$
$$\times\left[\int_0^1\frac{[\rho(n_1,n_2)-\rho(-n_1,n_2)]}{(\omega_t-\omega_0-i\beta\delta\omega_t u-i\frac{1}{2}\Gamma)}\exp(-\beta\delta\omega_t\tau u)du+\int_1^\infty\frac{[\rho(n_1,n_2)-\rho(-n_2,n_1)]}{(\omega_t-\omega_0-i\beta\delta\omega_t u-i\frac{1}{2}\Gamma)}\exp(-\beta\delta\omega_t\tau u)du\right], \tag{5.17}$$

where

$$\rho(n_1,n_2)=\frac{1-\bar{n}(n_1,n_2)}{1+\bar{n}(n_1,n_2)}$$

and

$$\bar{n}(\pm n_1,n_2)=\left[\frac{\beta}{2\delta}\right]^{1/2}\left[\frac{\exp\left[\mp\frac{i\pi}{4}\right]\pm\gamma\left[\frac{2\beta}{\delta}\right]^{1/2}\sqrt{1\pm u}}{\sqrt{1\pm u}+i\gamma\exp\left[\mp\frac{i\pi}{4}\right]\left[\frac{\beta}{2\delta}\right]^{1/2}(1\pm 2u)}\right],$$

$$\bar{n}(-n_2,n_1)=\left[\frac{\beta}{2\delta}\right]^{1/2}\left[\frac{\exp\left[-\frac{i\pi}{4}\right]-\gamma\left[\frac{2\beta}{\delta}\right]^{1/2}\sqrt{u-1}}{\sqrt{u-1}-i\gamma\exp\left[-\frac{i\pi}{4}\right]\left[\frac{\beta}{2\delta}\right]^{1/2}(2u-1)}\right]$$

for Kiselev's ABC.

We evaluate $R_1(\tau)$ numerically for parameters appropriate to CdS and CuCl crystals. The results are displayed in Figs. 5 and 6 for various ABC's, for the case of exact resonance: $\omega_0=\omega_t$. At a time $\tau=0$, when the trailing edge of the reflected pulse has just passed and steady-state reflectivity has dropped to zero, $|R_1(0)|^2$ is about 0.01–0.1 % of the incident intensity, depending on the choice of ABC. As τ increases, $|R_1(\tau)|^2$ begins to decrease exponentially, but at about $\tau\approx 1$ psec a crossover from an exponential to a slow power-law decay takes place. The resulting tail shows that the on-resonance nonlocal transient reflectivity persists for a few psecs after the reflected pulse is cut off. The results are qualitatively the same for all ABC's, but they differ quantitatively, depending on the choice of ABC and the material.

Resonant enhancement of nonlocal transient reflectivity is another remarkable feature and is illustrated in Figs. 7 and 8 for CdS and CuCl crystals. At fixed time $\tau=0.1$ psec, $|R_1(\omega_0)|$ is shown as a function of the laser frequency ω_0 in the vicinity of the exciton-resonance frequency ω_t. Enhancement of $|R_1(\omega_0)|^2$ by a factor 2–10 for various ABC's is observed in a narrow frequency range.

The nonlocal part of transient reflectivity decreases when the effective exciton-polariton mass m^* is increasing (or when the spatial-dispersion coefficient δ decreases). In this case, CuCl curves are quantitatively smaller in magnitude than the curves for CdS crystals, because of the higher effective mass for CuCl crystals. Especially, in the limit of infinite mass (local optics $\delta=0$), nonlocal transient reflectivity vanishes. We now consider the local part $E_L(\tau)$ modified by spatial dispersion.

VI. LOCAL PART OF TRANSIENT REFLECTIVITY

In this section we simplify the local part of transient reflectivity $E_L(\tau)$ [Eqs. (4.14) and (4.15)] following the procedure of Sec. V and discuss various features numerically for CdS and CuCl crystals. For this purpose we need to evaluate n_1, n_2, and n_+ at frequency $\omega=\omega_t+p\omega_t u-i\frac{1}{2}\Gamma$. Using Eqs. (A4)–(A6) to the leading order in δ, we obtain

$$n_{2,1}=+[a\pm(a^2-\epsilon_0 b)^{1/2}]^{1/2}, \tag{6.1}$$

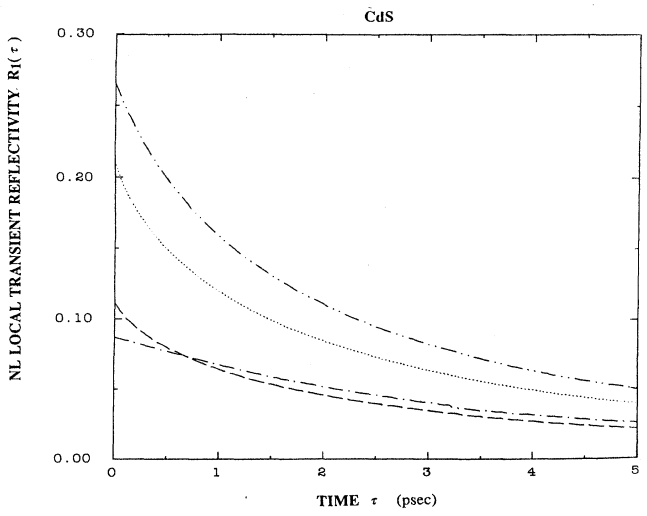

FIG. 5. Time decay of the nonlocal part of transient reflectivity $|R_1(\tau)|$ for various ABC's for the case of exact resonance $\omega_0=\omega_t$. The parameters for CdS are the same as in Fig. 3.

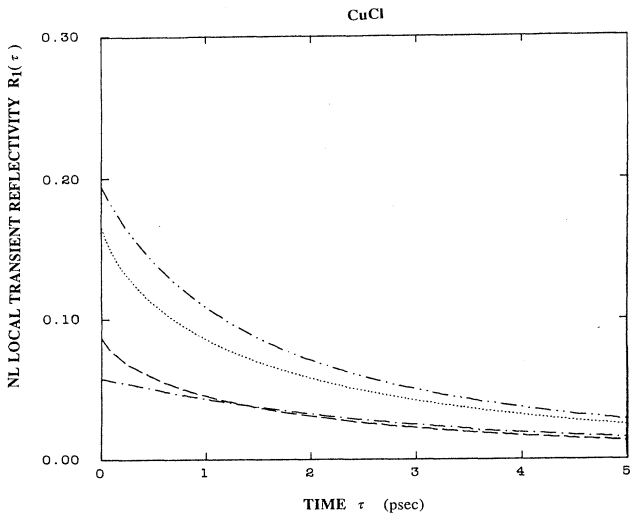

FIG. 6. Time decay of the nonlocal part of transient reflectivity $|R_1(\tau)|$ for various ABC's for the case of exact resonance $\omega_0=\omega_t$. The parameters for CuCl are the same as in Fig. 4.

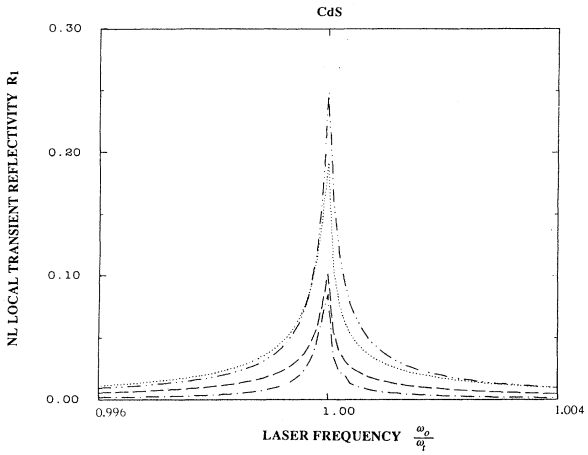

FIG. 7. Resonance enhancement of the nonlocal part of transient reflectivity $|R_1(\omega_0)|$ for various ABC's at fixed time $\tau=0.1$ psec. The parameters for CdS are the same as in Fig. 3.

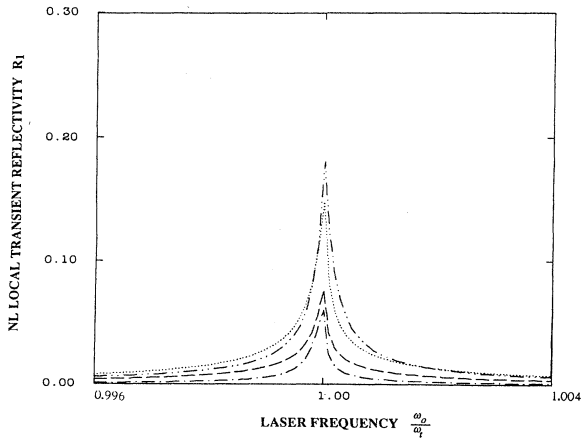

FIG. 8. Resonance enhancement of the nonlocal part of transient reflectivity $|R_1(\omega_0)|$ for various ABC's at fixed time $\tau=0.1$ psec. The parameters for CuCl are the same as in Fig. 4.

$$n_+ = +(2a-\epsilon_0)^{1/2}\,, \tag{6.2}$$

where

$$a \cong \left[\frac{\epsilon_0}{2}-\frac{pu}{\delta^2}\right],\quad b \cong \frac{2pu}{\delta^2}-\frac{\beta^2}{(\delta^2\epsilon_0)} \tag{6.3}$$

and $p=\beta^2/2\epsilon_0$.

Substituting Eq. (6.3) in (6.1) and (6.2) and assuming $\epsilon_0\delta^2/2p \ll 1$, we obtain

$$n_1 = \left[\epsilon_0\left[1-\frac{1}{u}\right]\right]^{1/2}, \tag{6.4}$$

$$n_2 = \left[\frac{\beta}{\delta}\right]\left[\frac{u}{\epsilon_0}\right]^{1/2}\left[1+\frac{1}{2}\left[\frac{\delta\epsilon_0}{\beta u}\right]^2\right], \tag{6.5}$$

$$n_+ = \left[\frac{\beta}{\delta}\right]\left[\frac{u}{\epsilon_0}\right]^{1/2}. \tag{6.6}$$

Using Eqs. (3.4) and (6.4)–(6.6) the effective refractive index for each ABC is found to be given by

$$\bar{n}(n_1,n_2) = \left[\epsilon_0\left[1-\frac{1}{u}\right]\right]^{1/2} \times\left[1+\left[\frac{\delta\epsilon_0}{\beta u}\right](u-1)^{-1/2}\right], \tag{6.7a}$$

$$\bar{n}(-n_1,n_2) = -\left[\epsilon_0\left[1-\frac{1}{u}\right]\right]^{1/2} \times\left[1-\left[\frac{\delta\epsilon_0}{\beta u}\right](u-1)^{-1/2}\right], \tag{6.7b}$$

for Pekar's ABC,

$$\bar{n}(n_1,n_2,n_+) = \left[\epsilon_0\left[1-\frac{1}{u}\right]\right]^{1/2} \times\left[1+\frac{1}{2}\left[\frac{\delta\epsilon_0}{\beta u}\right](u-1)^{-1/2}\right], \tag{6.8a}$$

$$\bar{n}(-n_1,n_2,n_+) = -\left[\epsilon_0\left[1-\frac{1}{u}\right]\right]^{1/2} \times\left[1-\frac{1}{2}\left[\frac{\delta\epsilon_0}{\beta u}\right](u-1)^{-1/2}\right], \tag{6.8b}$$

for Birman's ABC,

$$\bar{n}(n_1,n_2) = \left[\epsilon_0\left[1-\frac{1}{u}\right]\right]^{1/2}\left[1-\left[\frac{\delta\epsilon_0}{\beta}\right]^2\frac{1}{\left[u^2+\left[\frac{\delta\epsilon_0}{\beta}\right]^2\right]}\right], \tag{6.9a}$$

$$\bar{n}(-n_1,n_2) = -\left[\epsilon_0\left[1-\frac{1}{u}\right]\right]^{1/2}\left[1-\left[\frac{\delta\epsilon_0}{\beta}\right]^2\frac{1}{\left[u^2+\left[\frac{\delta\epsilon_0}{\beta}\right]^2\right]}\right], \tag{6.9b}$$

for Ting's ABC, and

$$\bar{n}(n_1,n_2)=\left[\epsilon_0\left[1-\frac{1}{u}\right]\right]^{1/2}\left[1+i\gamma-i\gamma\left[\frac{\delta\epsilon_0}{\beta}\right]^2\frac{1}{\left[u^2+\left[\frac{\delta\epsilon_0}{\beta}\right]^2\right]}\right], \tag{6.10a}$$

$$\bar{n}(-n_1,n_2)=-\left[\epsilon_0\left[1-\frac{1}{u}\right]\right]^{1/2}\left[1+i\gamma-i\gamma\left[\frac{\delta\epsilon_0}{\beta}\right]^2\frac{1}{\left[u^2+\left[\frac{\delta\epsilon_0}{\beta}\right]^2\right]}\right], \tag{6.10b}$$

for Kiselev's ABC.

Equations (3.3) and (6.7)–(6.10) are used to evaluate the integrands in Eqs. (4.14) and (4.15). By assuming $(\beta/\delta)\gg 1$ and using Eq. (4.18), $E_L(\tau)$ has the form

$$\mathrm{Re}[E_L(\tau)]=|R_2(\tau)|\sin(\omega_t\tau-\phi_2)\ , \tag{6.11}$$

where $R_2(\tau)=|R_2(\tau)|\exp[i\phi_2(\tau)]$ is given by

$$R_2(\tau)=i\exp(-i\omega_t\tau)\exp(-\tfrac{1}{2}\Gamma\tau)\left[\frac{2p\omega_t}{\pi(\epsilon_0)^{1/2}}\right]\times\left[\int_0^1 du\frac{\exp(-ip\omega_t\tau u)}{(\omega_t-\omega_0+p\omega_t u-i\frac{1}{2}\Gamma)}\frac{(u-u^2)^{1/2}}{\left[1-\frac{(\epsilon_0-1)}{\epsilon_0}u\right]}F(u)\right], \tag{6.12}$$

where

$$F(u)=1-\frac{2\delta}{\beta}\left[\frac{\epsilon_0}{u}\right]^{1/2}\frac{1}{\left[1-\frac{\epsilon_0-1}{\epsilon_0}u\right]} \tag{6.12a}$$

for Pekar's ABC,

$$F(u)=1-\frac{\delta}{\beta}\left[\frac{\epsilon_0}{u}\right]^{1/2}\frac{1}{\left[1-\frac{\epsilon_0-1}{\epsilon_0}u\right]} \tag{6.12b}$$

for Birman's ABC,

$$F(u)=1-\left[\frac{\epsilon_0\delta}{\beta}\right]^2\frac{1}{\left[u^2+\left[\frac{\epsilon_0\delta}{\beta}\right]^2\right]}\times\frac{\left[1-\frac{(\epsilon_0+1)}{\epsilon_0}u\right]}{\left[1-\frac{(\epsilon_0-1)}{\epsilon_0}u\right]} \tag{6.12c}$$

for Ting's ABC, and

$$F(u)=1-\left[\frac{\epsilon_0\delta}{\beta}\right]^2\frac{1}{\left[u^2+\left[\frac{\epsilon_0\delta}{\beta}\right]^2\right]}\times\frac{\left[1-\frac{(\epsilon_0+1)}{\epsilon_0}u\right]-\frac{2iu}{\gamma\epsilon_0}}{\left[1-\frac{(\epsilon_0-1)}{\epsilon_0}u\right]} \tag{6.12d}$$

for Kiselev's ABC.

Equations (6.12) show how the local part $R_2(\tau)$ of transient reflectivity is affected by spatial dispersion. We first consider the case of exact resonance, at $\omega_0=\omega_t$. Figures 9 and 10 show the time decay of $|R_2(\tau)|$ for parameters appropriate to CdS and CuCl crystals, respectively. By a solid line, we also show the corresponding curves obtained for a local medium ($\delta=0$). A close look shows that the effect of spatial dispersion reduces $|R_2(\tau)|$ and damps out its variation with time faster than the local

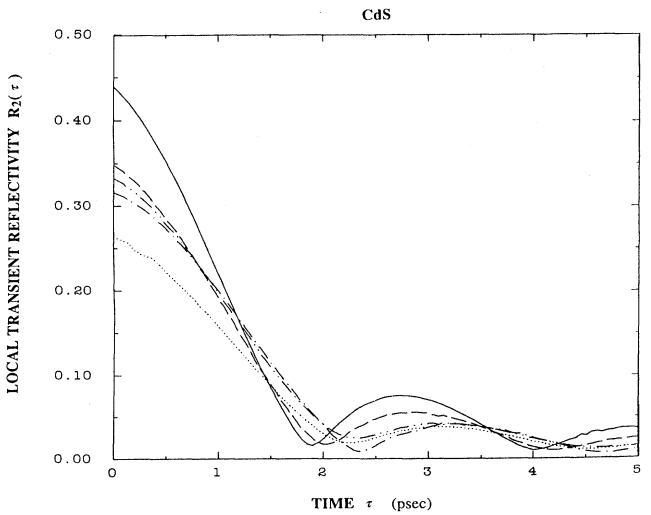

FIG. 9. Time oscillatory decay of the local part of transient reflectivity $|R_2(\tau)|$ for various ABC's for the case of exact resonance $\omega_0=\omega_t$. The parameters for CdS are the same as in Fig. 3.

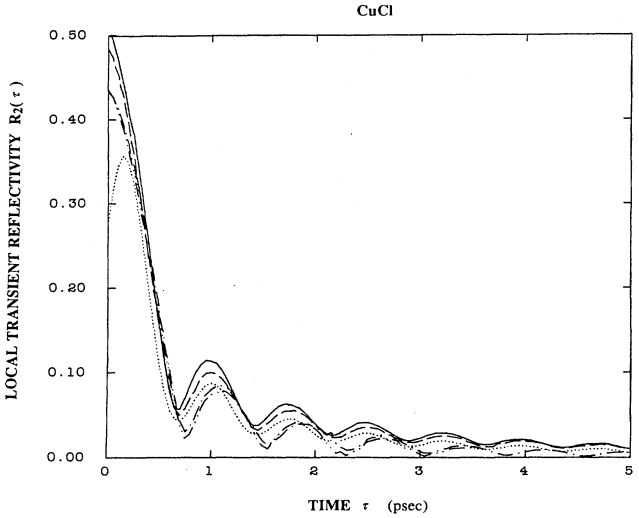

FIG. 10. Time oscillatory decay of the local part of transient reflectivity $|R_2(\tau)|$ for various ABC's for the case of exact resonance $\omega_0=\omega_t$. The parameters for CuCl are the same as in Fig. 4.

case (Elert's result). The rate of oscillations depends on the ω_{LT} (longitudinal-transverse) splitting of the material; CuCl shows faster oscillatory behavior than CdS for the same Γ/ω_t, since for CuCl, $\omega_{LT}=5.7$ meV, while for CdS, $\omega_{LT}=2$ meV. When we compare Figs. 9 and 10 with Figs. 5 and 6, respectively, we note that $|R_2(\tau)|^2$ is larger than $|R_1(\tau)|^2$ by about 4–10 times. Spatial dispersion reduces $|R_2(\tau)|$ for Pekar's and Birman's ABC (first order in δ), while $|R_2(\tau)|$ is almost close to local case ($\delta=0$) for Ting's and Kiselev's ABC (second order in δ).

Resonant enhancement of local transient reflectivity is shown in Figs. 11 and 12 for CdS and CuCl crystals. At fixed time $\tau=0.1$ psec, $|R_2(\omega_0)|$ is shown as a function of the laser frequency ω_0 in the vicinity of the exciton-resonance frequency ω_t. For comparison, we also show

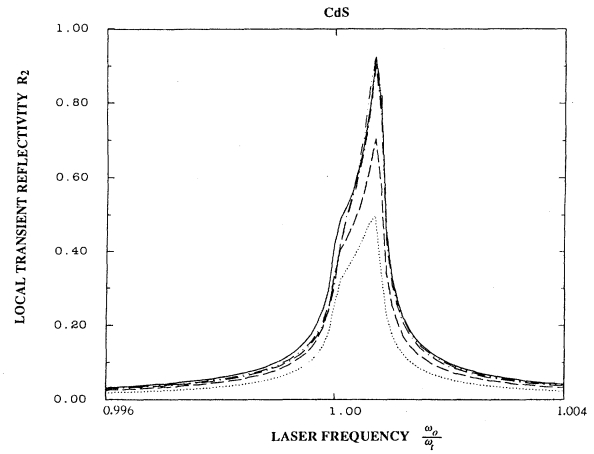

FIG. 11. Resonance enhancement of the local part of transient reflectivity $|R_2(\omega_0)|$ for various ABC's at fixed time $\tau=0.1$ psec. The parameters for CdS are the same as in Fig. 3.

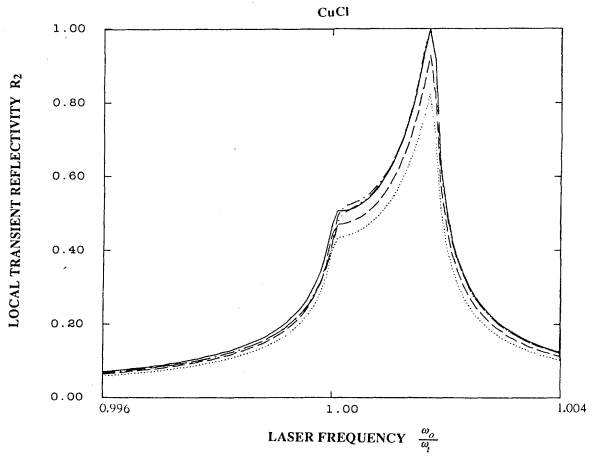

FIG. 12. Resonance enhancement of the local part of transient reflectivity $|R_2(\omega_0)|$ for various ABC's at fixed time $\tau=0.1$ psec. The parameters for CuCl are the same as in Fig. 4.

the corresponding curves obtained for a local medium ($\delta=0$). The peak of $|R_2(\omega_0)|$ is now, at ω_l, instead of ω_t, as it was in the case of $|R_1(\omega_0)|$. A remarkable difference between CdS and CuCl crystals is that the latter shows a richer structure for $|R_2(\omega_0)|$; we observe in Fig. 12 that for CuCl an additional local maximum at ω_t exists for all ABC's and local case, which cannot be detected for CdS crystals. The difference lies in the different values of the material parameters such as p, ω_t, and ϵ_0. Their combination in Eq. (6.7) is more enhanced for CuCl crystals. A physical explanation is given in Sec. VII.

VII. TOTAL TRANSIENT REFLECTIVITY

In Figs. 13 and 14 we give the time behavior of total transient reflectivity $|R_1(\tau)+R_2(\tau)|$ at resonance $\omega_0=\omega_t$ for CdS and CuCl crystals, respectively which shows the combined effect of local and nonlocal parts. The total reflectivity decays in a few psecs, but local part is stronger and dominates. Oscillatory behavior is faster for CuCl material than CdS because CuCl has larger β^2 (oscillator strength) than CdS. Both material show damped oscillatory behavior, but CdS has slower decay for the same Γ/ω_t and significant quantitative differences between different ABC's compared to CuCl. So CdS can be a good candidate to observe the time evolution of transient reflectivity. The oscillatory behavior in the local part can be understood due to the fact that for small Γ and fast cutoff time of the pulse, the response time of the electric dipoles arises in a distinct way.[30–32] However, in the case of the nonlocal part, we do not see the oscillations due to the finite effective exciton-polariton mass. With increase of damping Γ (for shorter relaxation times), the reflected pulse energy dissipates through damping process exponentially very fast without oscillations.

For fixed time $\tau=0.1$ psec, around the vicinity of exciton-polariton resonance ω_t, we plot total reflectivity

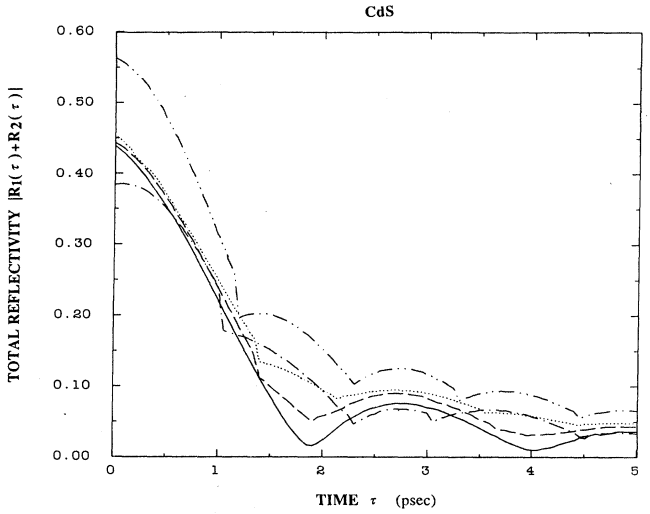

FIG. 13. Time oscillatory decay of the total transient reflectivity $|R_1(\tau)+R_2(\tau)|$ for various ABC's for the case of exact resonance $\omega_0=\omega_t$. The parameters for CdS are the same as in Fig. 3.

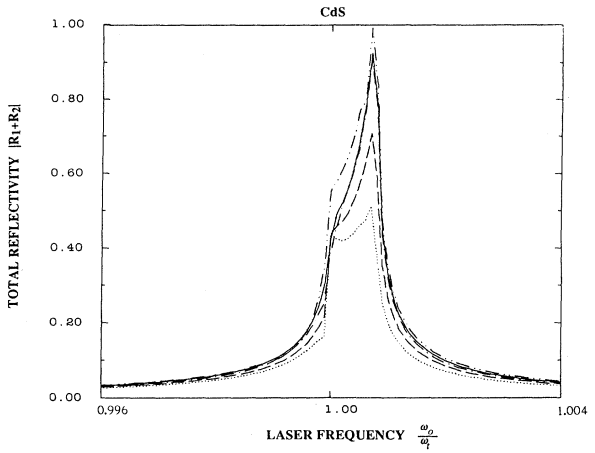

FIG. 15. Resonance enhancement of the total transient reflectivity $|R_1(\omega_0)+R_2(\omega_0)|$ for various ABC's at fixed time $\tau=0.1$ psec. The parameters for CdS are the same as in Fig. 3.

$|R_1(\omega_0)+R_2(\omega_0)|$ versus laser frequency ω_0 for CdS and CuCl crystals, respectively (see Figs. 15 and 16). Spatial dispersion reduces the total amplitude for all ABC's, while the local part still dominates. A remarkable result for CuCl material is the combined effect of local and nonlocal parts that enhances even more the double peak we find for local transient reflectivity for all ABC's and local case ($\delta=0$). In contrast CdS material which does not show any double peak for the local transient reflectivity case now shows it only for Pekar's ABC. Preliminary results for CdS (Ref. 33) assigned this double-peak behavior to the specific form of Pekar's ABC, but CuCl shows that this qualitative behavior prevails for all ABC's and even for the local scale ($\delta=0$). A possible explanation for this phenomenon could be the broader gap for CuCl ($\omega_{LT}=5.7$ meV) compared to the CdS case ($\omega_{LT}=2$ meV) that permits one to see the richer structure of transient reflectivity in the vicinity of ω_t. This structure could be assigned to exciton-polaritons group velocity decrease in the gap.[34] Exciton polaritons are heavily damped in this region, which slows down their motion. For this reason, CuCl is a good candidate to investigate transient reflectivity in the vicinity of ω_t.

VIII. CONCLUSIONS

We have carried out analytical and numerical calculations for the reflectivity of an EM pulse of duration T

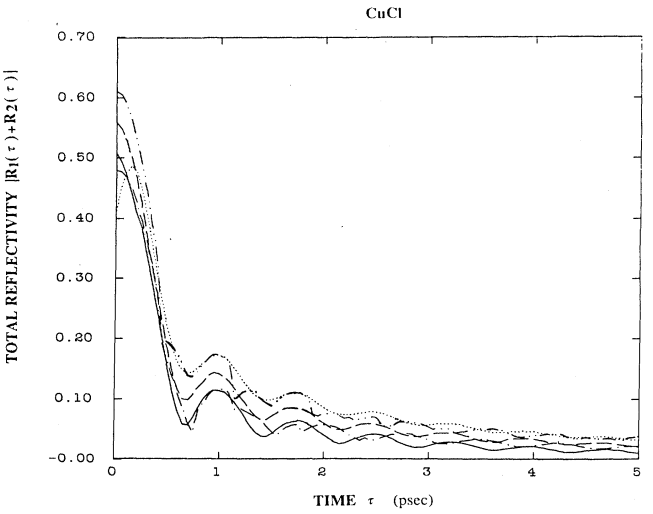

FIG. 14. Time oscillatory decay of the total transient reflectivity $|R_1(\tau)+R_2(\tau)|$ for various ABC's for the case of exact resonance $\omega_0=\omega_t$. The parameters for CuCl are the same as in Fig. 4.

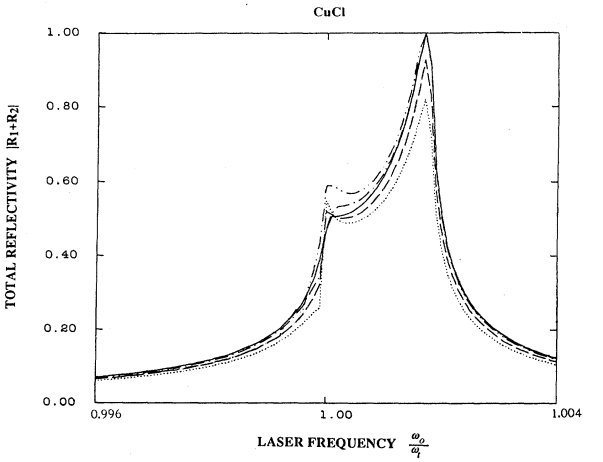

FIG. 16. Resonance enhancement of the total transient reflectivity $|R_1(\omega_0)+R_2(\omega_0)|$ for various ABC's at fixed time $\tau=0.1$ psec. The parameters for CuCl are the same as in Fig. 4.

from a spatially-dispersive semi-infinite medium for the case of normal incidence. We investigated the role of different ABC's on the steady-state reflectivity and transient reflectivity. Especially, in the time domain, after the pulse cutoff, the medium continues emitting energy in damped oscillatory form for the case of long relaxation times (small Γ). Different ABC's influence the decay process in different quantitative ways, especially for laser frequency ω_0 very close to the exciton-polariton resonance frequency ω_t, where spatial-dispersion effects are dominant. In the frequency domain, the transient-reflectivity amplitude shows double peak at ω_t and ω_l, for some or all ABC's depending on the choice of material.

Our results are obtained under certain simplifying assumptions. The finite-length crystal is replaced by a semi-infinite nonlocal medium. Furthermore, we have simplified our calculations by assuming dimensionless parameters $\delta=(\hbar\omega_t/m^*c^2)^{1/2}$, $p=\beta^2/2\epsilon_0$, Γ/ω_t to be small. For CdS and CuCl crystals each of them is $\leq 10^{-3}$.

Measurements of predicted features of transient reflectivity can provide independently determined values of important exciton-polariton values such as mass, lifetime, oscillator strength, ω_t, and ω_l plus an experimental verification of the "true" ABC for CdS and CuCl crystals.

In reality, experiments are designed for oblique geometries. An extension of this analysis for oblique transient reflectivity for various ABC's will be presented in a subsequent paper.[35]

Note added in proof. Numerical analysis for Gaussian picosecond pulses at normal incidence and at Brewster's angle was reported by J. Aavishoo, J. Lipmaa, and J. Kuhl [J. Opt. Soc. Am. B **5**, 1631 (1988)]. To our knowledge, the first experimental verification for transient reflectivity of picosecond Gaussian pulses for spatially dispersive media (GaAs) was reported by J. Aavishoo and J. Kuhl (unpublished).

ACKNOWLEDGMENTS

This work was supported in part by the Naval Air System Command under Grant No. 19-87-G-0251 and Faculty Research Awards Program, Professional Staff Congress, City University of New York. One of us (S.V.B.) would like to specially thank A. Puri and G. P. Agrawal for discussion during the preliminary parts of this work and P. Lavallard, C. Gourdon, C. Hirleman, J. P. Morhange, and N. Piccioli for discussions during a short visit at Université de Paris–VI.

APPENDIX: CONTOUR-INTEGRATION METHOD TO EVALUATE THE REFLECTED FIELD [EQ. (3.6)]

In this Appendix we outline the algebraic details to evaluate the integral in Eq. (3.6) in the complex ω plane for $t\geq 2L/c$. It is helpful to break the integral in two parts arising from each term in the curly brackets: $\{1-\exp[i(\omega-\omega_0)T]\}$. The first part contributes for $t>2L/c$ while the second part contributes only for $t>2L/c+T$. Equation (3.6) can therefore be written in the form

$$E_R(t)=\mathrm{Re}[E(t-2L/c)\Theta(t-2L/c) - \exp(-i\omega_0 T)E(t-2L/c-T) \times\Theta(t-2L/c-T)] , \tag{A1}$$

where

$$E(\tau)=\lim_{\eta\to 0}\int_{-\infty}^{+\infty} f(n_1,n_2)d\omega \tag{A2a}$$

for the ABC's of Pekar, Ting, and Kiselev, and

$$E(\tau)=\lim_{\eta\to 0}\int_{-\infty}^{+\infty} f(n_1,n_2,n_+)d\omega \tag{A2b}$$

for Birman's ABC, while

$$\left.\begin{matrix} f(n_1,n_2) \\ f(n_1,n_2,n_+) \end{matrix}\right\}=\frac{1}{2\pi}\frac{\rho(\omega)}{\omega_0-\omega-i\eta}\exp(-i\omega\tau),\quad \tau>0 . \tag{A3}$$

For notational convenience, we have explicitly shown the dependence of the integrands $f(n_1,n_2)$ and $f(n_1,n_2,n_+)$ on the refractive indices n_1, n_2, and n_+ [see Eq. (3.3)] and the ω dependence is implicitly understood.

The choice of the appropriate contour depends on the singularities of $f(n_1,n_2)$ and $f(n_1,n_2,n_+)$. For this purpose we require an explicit form of n_1, n_2, and n_+. Using Eq. (3.2) in (3.5), we obtain

$$n_{2,1}=+[a\pm(a^2-\epsilon_0 b)^{1/2}]^{1/2} , \tag{A4}$$

$$n_+=+(2a-\epsilon_0)^{1/2} , \tag{A5}$$

$$\begin{aligned} a&=(2\omega^2\delta)^{-1}[\epsilon_0\omega^2\delta^2+(\omega^2-\omega_t^2-i\omega\Gamma)] , \\ b&=(\omega^2\delta^2)^{-1}\left[(\omega^2-\omega_t^2-i\omega\Gamma)-\frac{\beta^2\omega_t^2}{\epsilon_0}\right] , \end{aligned} \tag{A6}$$

where

$$\beta^2=(4\pi\alpha_0),\quad \delta^2=\left[\frac{\hbar\omega_t}{m^*c^2}\right] .$$

An examination of Eq. (A4) shows that the conditions $b=0$ and $a^2=\epsilon_0 b$ correspond to the branch-point singularities in $f(n_1,n_2)$. A further examination in Eq. (A5) reveals an additional condition $2a=\epsilon_0$, which corresponds to the branch-point singularities in $f(n_1,n_2,n_+)$, in addition to the two previous ones.

Using Eq. (A6), the first two complex conditions yield six branch points (in the complex ω plane) ω_j, $j=1-6$, whose location is given by Eqs. (4.1)–(4.3), while all three conditions yield eight branch points ω_j, $j=1-8$, whose location is given by Eqs. (4.1)–(4.4). So, the main difference between $f(n_1,n_2)$ and $f(n_1,n_2,n_+)$ is the number of branch points for each one.

The branch points ω_1 and ω_2 arise from the condition $b=0$. Around these points the integrands $f(n_1,n_2)$ and $f(n_1,n_2,n_+)$ are made single valued by going to the Riemann sheet on which $n_1\to -n_1$ and n_2,n_+ remain unchanged.

The branch points ω_3, ω_4, ω_5, and ω_6 arise from the

condition $a^2=\varepsilon_0 b$; on the corresponding Riemann sheet, n_1 and n_2 are interchanged ($n_1 \rightarrow n_2$) and n_+ remains unchanged.

The branch points ω_7 and ω_8 arise from the condition $2a=\varepsilon_0$; in this case, $f(n_1,n_2,n_+)$ is made single valued by going to the Riemann sheet on which $n_+ \rightarrow -n_+$ and n_1,n_2 remain unchanged.

The appropriate contours to evaluate Eqs. (A2) and (A3) are shown in Figs. 2(a) and 2(b) and contain only a single pole at $\omega=\omega_0-i\eta$ for both cases.

A straightforward application of Cauchy's theorem shows that

$$\oint f(n_1,n_2)d\omega=\int_{-\infty}^{+\infty} f(n_1,n_2)d\omega+\int_{\omega_3}^{\omega_1}[f(n_1,n_2)-f(-n_1,n_2)]d\omega + \int_{\omega_3}^{\mathrm{Re}\omega_3-i\infty}[f(-n_2,n_1)-f(n_1,n_2)]d\omega+\int_{\omega_4}^{\omega_2}[f(-n_1,n_2)-f(n_1,n_2)]d\omega + \int_{\omega_4}^{\mathrm{Re}\omega_4-i\infty}[f(n_1,n_2)-f(-n_2,n_1)]d\omega=2\pi i\,\mathrm{Res}_1 \tag{A7}$$

and

$$\begin{aligned}\oint f(n_1,n_2,n_+)d\omega=&\int_{-\infty}^{+\infty} f(n_1,n_2,n_+)d\omega+\int_{\omega_3}^{\omega_1}[f(n_1,n_2,n_+)-f(-n_1,n_2,n_+)]d\omega\\ &+\int_{\omega_3}^{\mathrm{Re}\omega_3-i\infty}[f(-n_2,n_1,-n_+)-f(n_1,n_2,n_+)]d\omega\\ &+\int_{\omega_7}^{\omega_1}[f(n_1,n_2,n_+)-f(-n_1,n_2,n_+)]d\omega\\ &+\int_{\omega_4}^{\omega_8}[f(-n_1,n_2,-n_+)-f(n_1,n_2,n_+)]d\omega\\ &+\int_{\omega_4}^{\mathrm{Re}\omega_4-i\infty}[f(n_1,n_2,n_+)-f(-n_2,n_1,-n_+)]d\omega\\ &+\int_{\omega_8}^{\omega_2}[f(-n_1,n_2,n_+)-f(n_1,n_2,n_+)]d\omega=2\pi i\,\mathrm{Res}_2\ ,\end{aligned} \tag{A8}$$

where $\mathrm{Res}_1,\mathrm{Res}_2$ represent the residues of $f(n_1,n_2)$ and $f(n_1,n_2,n_+)$ at the pole $\omega=\omega_0-i\eta$, respectively. Using Eqs. (A2) and (A7) or (A8), we formally decompose $E(\tau)$ into a steady state (pole contribution) and the transient (branch-point contribution) parts,

$$E(\tau)=E_S(\tau)+E_T(\tau)\ , \tag{A9}$$

where

$$E_S(\tau)=-i\rho(\omega_0)\exp(-i\omega_0\tau) \tag{A10}$$

for all ABC's and

$$E_T(\tau)=\int_{\omega_3}^{\omega_1} g(\omega)d\omega-\int_{\omega_4}^{\omega_2} g(\omega)d\omega - \int_{\omega_3}^{\mathrm{Re}\omega_3-i\infty} g'(\omega)d\omega+\int_{\omega_4}^{\mathrm{Re}\omega_4-i\infty} g'(\omega)d\omega \tag{A11}$$

for the ABC's of Pekar, Ting, and Kiselev,

$$\begin{aligned}E_T(\tau)=&\int_{\omega_3}^{\omega_7} g_1(\omega)d\omega-\int_{\omega_4}^{\omega_8} g_1(\omega)d\omega\\ &-\int_{\omega_3}^{\mathrm{Re}\omega_3-i\infty} g''(\omega)d\omega+\int_{\omega_4}^{\mathrm{Re}\omega_4-i\infty} g''(\omega)d\omega\\ &+\int_{\omega_7}^{\omega_1} g_2(\omega)d\omega-\int_{\omega_8}^{\omega_2} g_2(\omega)d\omega\end{aligned} \tag{A12}$$

for Birman's ABC, while

$$g(\omega)=[f(-n_1,n_2)-f(n_1,n_2)]\ , \tag{A13a}$$

$$g'(\omega)=[f(-n_2,n_1)-f(n_1,n_2)]\ , \tag{A13b}$$

$$g_1(\omega)=[f(-n_1,n_2,-n_+)-f(n_1,n_2,n_+)]\ , \tag{A14a}$$

$$g_2(\omega)=[f(-n_1,n_2,n_+)-f(n_1,n_2,n_+)]\ , \tag{A14b}$$

$$g''(\omega)=[f(-n_2,n_1,-n_+)-f(n_1,n_2,n_+)]\ . \tag{A14c}$$

We have found it useful to further decompose the transient part $E_T(\tau)$ into a "local" part and a "nonlocal" part. This facilitates comparison with a local medium for which the nonlocal part, by definition, vanishes identically. Such a decomposition can be carried out by noting for $f(n_1,n_2)$ that for a local medium the branch-out line (joining ω_1 and ω_3) in Fig. 2(a) is horizontal. For the case of $f(n_1,n_2,n_+)$ the branch-cut line (joining ω_1 and ω_7) in Fig. 2(b) shrinks into the point ω_7. This can be easily verified using Eqs. (4.1), (4.2), and (4.4) with $\delta=0$. We then formally obtain

$$E_T(\tau)=E_L(\tau)+E_{\mathrm{NL}}(\tau) \tag{A15}$$

for all ABC's, while

$$E_L(\tau)=\int_{\mathrm{Re}\omega_3+i\,\mathrm{Im}\omega_1}^{\omega_1} g(\omega)d\omega-\int_{\mathrm{Re}\omega_4+i\,\mathrm{Im}\omega_1}^{\omega_2} g(\omega)d\omega\ , \tag{A16}$$

$$E_{\mathrm{NL}}(\tau)=\int_{\omega_3}^{\mathrm{Re}\omega_3+i\,\mathrm{Im}\omega_1} g(\omega)d\omega-\int_{\omega_4}^{\mathrm{Re}\omega_4+i\,\mathrm{Im}\omega_2} g(\omega)d\omega - \int_{\omega_3}^{\mathrm{Re}\omega_3-i\infty} g'(\omega)d\omega+\int_{\omega_4}^{\mathrm{Re}\omega_4-i\infty} g'(\omega)d\omega\ , \tag{A17}$$

for the ABC's of Pekar, Ting, and Kiselev, and

$$E_L(\tau)=\int_{\omega_7}^{\omega_1} g_2(\omega)d\omega-\int_{\omega_8}^{\omega_2} g_2(\omega)d\omega\ , \tag{A18}$$

$$E_{\rm NL}(\tau)=\int_{\omega_3}^{\omega_7} g_1(\omega)d\omega-\int_{\omega_4}^{\omega_8} g_1(\omega)d\omega - \int_{\omega_3}^{{\rm Re}\omega_3-i\infty} g''(\omega)d\omega+\int_{\omega_4}^{{\rm Re}\omega_4-i\infty} g''(\omega)d\omega \tag{A19}$$

for Birman's ABC. We not substitute $E=E_S+E_L+E_{\rm NL}$ in Eq. (A1) and obtain

$$E_R(0,t,\omega_0)={\rm Re}[\tilde{E}_S(t)+\tilde{E}_L(t)+\tilde{E}_{\rm NL}(t)]\ , \tag{A20}$$

where

$$\tilde{E}_S(t)=i\rho(\omega_0)[\Theta(t-2L/c)-\Theta(t-2L/c-T)]\times\exp[-i\omega_0(t-2L/c)]\ , \tag{A21}$$

$$\tilde{E}_T(t)=[E_j(t-2L/c)\Theta(t-2L/c) - \exp(-i\omega_0 T)E_j(t-2L/c-T)\times\Theta(t-2L/c-T)]\ , \tag{A22}$$

with j=NL or L.

The evaluation of Eqs. (A16)–(A19) can be simplified by noting that in most cases of practical interest the three parameters δ, p, and Γ/ω_t are much smaller than unity ($\leq 10^{-3}$). We are therefore justified in neglecting their products and higher powers. The branch points ω_j given by Eqs. (4.1)–(4.5) then simplify into the Eqs. (4.6)–(4.9).

Again as a reminder, we have defined $p=\beta^2/2\epsilon_0=2\pi\alpha_0/\epsilon_0$ and physically $p=(\omega_l-\omega_t)/\omega_t$, where $\omega_l-\omega_t$ is the so-called longitudinal-transverse LT splitting.

An appropriate change of variables permits us to rewrite the expressions in Eqs. (A16)–(A19) in the following simplified form:

$$E_L(\tau)=p\omega_t\left[\int_0^1 g(\omega_t+p\omega_t u-i\tfrac{1}{2}\Gamma)du+\int_0^1 g(-\omega_t+p\omega_t u-i\tfrac{1}{2}\Gamma)du\right]\ , \tag{A23}$$

$$E_{\rm NL}(\tau)=i\beta\delta\omega_t\left[\int_0^1 g(\omega_t-i\beta\delta\omega_t u-i\tfrac{1}{2}\Gamma)du-\int_0^1 g(-\omega_t-i\beta\delta\omega_t u-i\tfrac{1}{2}\Gamma)du + \int_1^\infty g'(\omega_t-i\beta\delta\omega_t u-i\tfrac{1}{2}\Gamma)du-\int_1^\infty g'(-\omega_t-i\beta\delta\omega_t u-i\tfrac{1}{2}\Gamma)du\right]\ , \tag{A24}$$

for the ABC's of Pekar, Ting, and Kiselev, and

$$E_L(\tau)=p\omega_t\left[\int_0^1 g_2(\omega_t+p\omega_t u-i\tfrac{1}{2}\Gamma)du+\int_0^1 g_2(-\omega_t+p\omega_t u-i\tfrac{1}{2}\Gamma)du\right]\ , \tag{A25}$$

$$E_{\rm NL}(\tau)=i\beta\delta\omega_t\left[\int_0^1 g_1(\omega_t-i\beta\delta\omega_t u-i\tfrac{1}{2}\Gamma)du-\int_0^1 g_1(-\omega_t-i\beta\delta\omega_t u-i\tfrac{1}{2}\Gamma)du + \int_1^\infty g''(\omega_t-i\beta\delta\omega_t u-i\tfrac{1}{2}\Gamma)du-\int_1^\infty g''(-\omega_t-i\beta\delta\omega_t u-i\tfrac{1}{2}\Gamma)du\right]\ , \tag{A26}$$

for Birman's ABC.

*Permanent address: Department of Physics, San Jose State University, 1 Washington Square, San Jose, CA 95192-0106.

[1]A review of various optical transient effects connected with local and nonlocal (spatially dispersive) media is given by A. Puri and J. L. Birman, in *Semiconductors Probed by Ultrafast Laser Spectroscopy*, edited by R. R. Alfano (Academic, New York, 1984), Chap. 22, Vol. II.

[2]E. L. Ivchenko, in *Excitons*, edited by E. I. Rashba and M. D. Sturge (North-Holland, New York, 1982), Chap. 4.

[3]A. Sommerfeld, Ann. Phys. (Leipzig) **44**, 177 (1914).

[4]L. Brillouin, *Wave Propagation and Group Velocity* (Academic, New York, 1960).

[5]M. Frankel and J. L. Birman, Phys. Rev. A **15**, 2000 (1977).

[6]E. Gitterman and M. Gitterman, Phys. Rev. A **13**, 763 (1976).

[7]L. A. Vainshtein, Usp. Fiz. Nauk **118**, 339 (1976) [Sov. Phys.—Usp. **19**, 189 (1976)].

[8]J. A. Gaspar-Amenta and P. Halevi, Opt. Commun. **64**, 217 (1987).

[9]J. S. Nkoma, J. Phys. C **16**, 3713 (1983).

[10]T. Skettrup, Phys. Status Solidi B **60**, 695 (1973).

[11]I. Broser, M. Rosenzweig, R. Broser, M. Richard, and E. Birkicht, Phys. Status Solidi B **90**, 77 (1978).

[12]D. Elert, Ann. Phys. (Leipzig) **7**, 65 (1930); J. C. Eilbeck, J. Phys. A **5**, 1355 (1972); I. H. Campbell and P. N. Fauchet, Opt. Lett. **13**, 634 (1988); S. V. Branis, U. Arya, and J. L. Birman, Bull. Am. Phys. Soc. **33**, 351 (1988).

[13]D. N. Pattanayak, G. P. Agrawal, and J. L. Birman Phys. Rev. Lett **46**, 174 (1981); G. P. Agrawal, J. L. Birman, D. N. Pattanayak, and A. Puri, Phys. Rev. B **25**, 2715 (1982).

[14]A review of the ABC problem for spatial dispersive medium is given by J. L. Birman, in *Excitons*, edited by E. I. Rashba and M. D. Sturge (North-Holland, New York, 1982), Chap. 2.

[15]S. I. Pekar, Zh. Eksp. Teor. Fiz. **33**, 1022 (1957) [Sov. Phys.—JETP **6**, 785 (1958)].

[16]J. J. Hopfield and D. G. Thomas, Phys. Rev. **132**, 563 (1963).

[17]K. L. Kliewer and R. Fuchs, Phys. Rev. **172**, 607 (1968); **185**, 905 (1969).

[18]D. L. Johnson and P. R. Rimbey, Phys. Rev. B **14**, 2398 (1976).

[19]V. A. Kiselev, Fiz. Tverd. Tela (Leningrad) [Sov. Phys.—

Solid State **15**, 2338 (1974)].
[20]J. J. Sein and J. L. Birman, Phys. Rev. B **6**, 2482 (1972); J. J. Sein, Ph.D. thesis, New York University, New York, 1969.
[21]A. A. Maradudin and D. L. Mills, Phys. Rev. B **7**, 2787 (1973).
[22]G. P. Agrawal, D. N. Pattanayak, and E. Wolf, Phys. Rev. Lett. **27**, 1022 (1971); Phys. Rev. B **10**, 1477 (1974).
[23]R. Zeyher, J. L. Birman, and W. Brenig, Phys. Rev. B **6**, 4613 (1972).
[24]C. S. Ting, M. Frankel, and J. L. Birman, Solid State Commun. **17**, 1285 (1975).
[25]T. Shigenari, X. Z. Lu, and H. Z. Cummins, Phys. Rev. B **30**, 1962 (1984).
[26]M. Dagenais and W. F. Sharfin, Phys. Rev. Lett. **58**, 1776 (1987).
[27]M. Kuwata, J. Phys. Soc. Jpn. **53**, 4456 (1984).
[28]P. Lavallard and C. Gourdon, Phys. Rev. B **31**, 6654 (1985).
[29]C. Gourdon, thèse de troisème cycle, Université de Paris–VI, Paris, France, 1984.
[30]J. E. Rothenberg, D. Grischkowsky, and A. C. Balant, Phys. Rev. Lett. **53**, 552 (1984).
[31]J. E. Rothenberg, IEEE J. Quantum Electron. **QE-22**, 174 (1986).
[32]B. Segard and B. Macke, Phys. Lett. **109A**, 213 (1985).
[33]S. V. Branis, K. Arya, and J. L. Birman, in *Ultrafast Lasers: Probe Phenomena in Bulk and Microstructure Semiconductors,* Vol. 793 of *SPIE Proceedings,* edited by R. R. Alfano (SPIE, Bellingham, WA, 1987); *Laser Optics of Condensed Matter,* edited by J. L. Birman, H. Z. Cummins, and A. A. Kaplyanskii (Plenum, New York, 1988).
[34]P. Lavallard (private communication).
[35]S. V. Branis, K. Arya, and J. L. Birman (unpublished).